

Performance summary of the Brookhaven superconducting power transmission system

E.B. Forsyth and R.A. Thomas

Brookhaven National Laboratory*, Associated Universities, Inc., Upton, NY 11973, USA

Received 12 June 1986

Following a study in 1971 at Brookhaven National Laboratory it was concluded that an optimal design for a superconducting power transmission system would utilize niobium-tin superconductor in flexible cables cooled by supercritical helium. A 1000 MVA prototype was constructed and operated from 1982 until the present. The operating performance of the cables, cable enclosure and terminations is summarized over a wide range of operating conditions. The results confirm the technical feasibility of this technology to move large blocks of electric power over long distances.

Keywords: superconductivity; Nb₃Sn; power transmission systems

Research and development on superconducting power transmission systems started at Brookhaven National Laboratory in 1971 when a study of the subject was made under a grant from the National Science Foundation (NSF)¹. At that time there were many development projects in Europe, the USSR, Japan and the USA. They included a wide range of technical options embracing both a.c. and d.c. transmission systems. The options under development included conductor material and design, type of electrical insulation, rigid and flexible cables, and both self-contained and independent types of cryogenic insulation. In the summer of 1972 laboratory work was started at Brookhaven to develop a transmission system which the NSF study had predicted to be the most technically attractive and cost effective. The important technical choices were as follows:

- 1 a conductor incorporating niobium-tin superconductor²;
- 2 a flexible cable installed in a rigid insulated enclosure³;
- 3 cooling by means of helium in the supercritical regime; and
- 4 an electrical insulation of lapped polymeric tape. The use of lapped tape insulation permits the cable to bend on a reel. The insulation is permeated by the coolant.

The history of the development cycle is shown in *Figure 1*. In the early years the effort concentrated on materials development and on system studies carried out in cooperation with electric utility companies. These studies were an important factor in the optimization of the engineering design. In 1975 construction started on an outdoor test site which would be capable of testing cables in an environment similar to a utility company application. The site was to be capable of testing cables with simultaneous voltage

and current excitation. After much debate a rating of 330 MVA per cable at 80 kV line-to-neutral was chosen, corresponding to a three phase rating of 138 kV, 1000 MVA. During the last half of the 1970s the emphasis moved away from materials R&D into the engineering design of the test site, the cables, and the cable terminations. The cables were built and installed in 1981 and power first applied in 1982; nearly 10 years after the start of development in the laboratory. Since 1982, the system has been operated on eight occasions for periods of 5–27 days; a view of the test site is shown in *Figure 2*.

The test site required six major components; the design and performance of three of these components are directly relevant to those needed for a commercial version of the system. The design of the other three components, or subsystems, are relevant to varying degrees. The six components are:

- 1 the superconducting cable. The design and performance of the cable is directly applicable to the construction of a cable for a commercial system. Two cables, each ≈ 115 m in length, have been tested. In practice it is anticipated that cables ≈ 1 km in length would be installed in one piece with a joint to the adjacent cables. Thus construction and installation problems which may get worse with increase in length must still be investigated. The Brookhaven test site does not include a cable joint. The development of a joint is discussed below;
- 2 cable termination. These devices are required to make the transition between the cryogenic and ambient temperature portions of the system. The electrical ratings must match those of the cables under test. The design and performance is highly relevant to a commercial product;
- 3 the cable enclosure. System studies performed early in the programme showed that the cable enclosure design had a significant impact on both capital and operating

*Operated by Associated Universities, Inc., under contract to the US Department of Energy

SCHEDULE OF ACTUAL DEVELOPMENT AT BNL

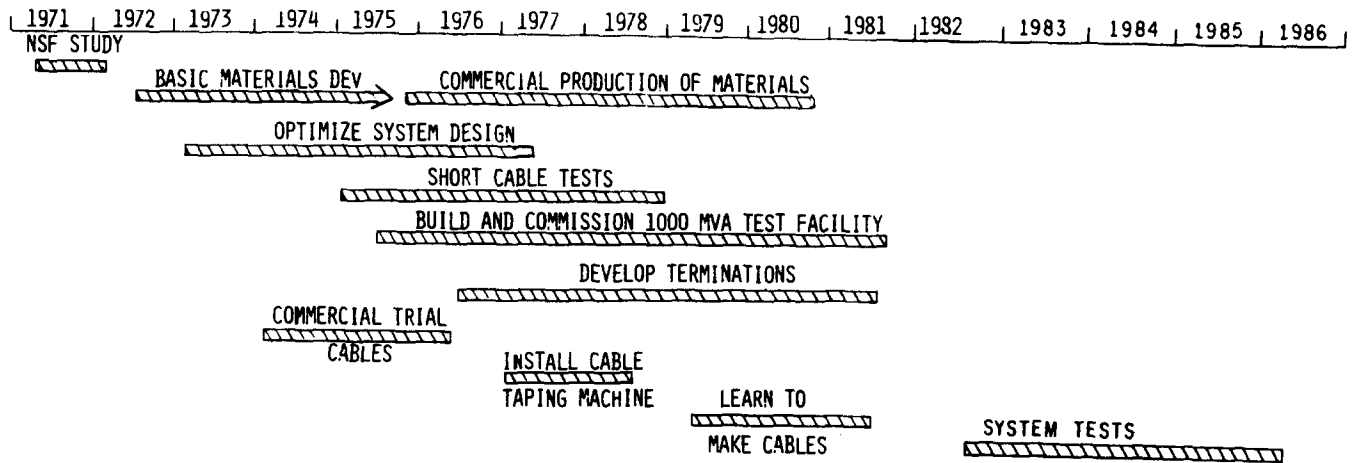


Figure 1 Areas of major activity during the development period of the superconducting power transmission system

- costs. The ratio of these costs is a very important design choice and depends on many factors including the specifics of the route itself, the cost of energy and the cost of money. The enclosure at Brookhaven is designed to minimize capital cost; the heat in-leak (a major factor in operating cost) is not the minimum that can be achieved;
- 4 the cryogenics system. Not all aspects of the system are applicable to a commercial design. The all-rotary refrigerator has many features intended to match utility company service but the method of cool-down would be quite different in actual systems which would be at least two orders of magnitude longer than the one under test;
 - 5 control system. The advent of versatile and low cost computer controls during the development period of the test site was very serendipitous. The control system permitted long periods of unattended operation which were not anticipated at the start of the programme. Although the performance of the control system is of great interest, and some valuable lessons were learned, it must be recognized that this is still a rapidly developing area and the controls for a commercial system would be designed with different objectives in mind; and

- 6 the electrical excitation system. This system would not be needed in a commercial application. However, the performance is of interest to researchers, and the grounding techniques are relevant to a future commercial design.

Superconducting cable performance

For convenience, the cable performance may be divided into three areas: mechanical, electrical and abnormal conditions. The mechanical performance covers bending, installation and thermal cycling of the cable. Electrical performance of interest includes the losses and critical current of the conductor, 60 Hz partial discharge inception level and the ability of the insulation to withstand impulses. Abnormal conditions mean conditions that may arise occasionally during operation which must not result in permanent damage to the cable system. Examples are operation with the conductor quenched, operation with the refrigerator shut down and operation with electrical overloads.

The design of the flexible cable has been adequately reported in the technical literature^{4,5}. An assembly drawing of the cable is shown in Figure 3. Briefly, the cable consists of many layers wound on an inner support mandrel which also provides a cooling channel. The inner conductor is formed by two pairs of helical tape windings. An inner pair with left and right-handed lay is oxygen-free copper with a total thickness of ≈ 0.75 mm (the cryostabilizer). The outer pair is also formed from two helical tapes with a pitch angle of $\approx 45^\circ$. Each tape is a laminate of stainless steel, niobium-tin and copper. The total thickness of the tape is 100 μ m. The inner conductor assembly is covered by an aluminized shielding tape and then the electrical insulating tape is applied. This is made from a bi-laminate of oriented polypropylene⁶. The insulation is also shielded on the outside, and the outer conductor assembly is similar to the inner conductor except wider tapes are used. The superconductive pair form the inner two layers of the outer conductor. The outer is insulated from ground by means of Kapton tapes. An armour layer is then put on to maintain mechanical integrity. The cooling system design requires a gas-tight cable jacket; this is provided by a corrugated stainless steel tube. The cable was pulled into the tube during installation but presumably it would be possible to apply this tube on the outside during cable manufacture, as is commonly done on conventional self-contained cables.

The pitch angles of the various cable components



Figure 2 East end of the test facility showing the air-entrance bushing of two terminations. The cable enclosure is left centre. The compensation supply can be seen between the terminations (see also Figure 17)

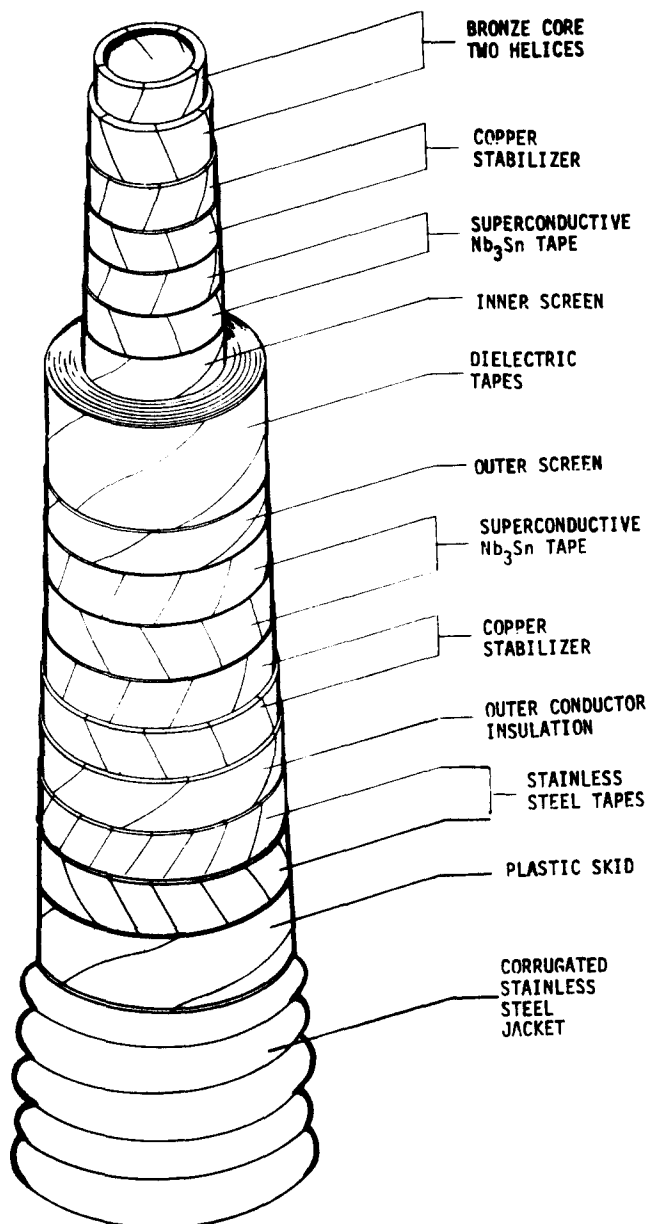


Figure 3 General assembly diagram of flexible superconducting power transmission cable design

are chosen to simultaneously satisfy both electrical and magnetic considerations and provide a means of accommodating contraction on cool-down. Fortunately, it turned out to be possible to meet these constraints so that each layer of the cable contracts the same distance radially on cool-down while maintaining a fixed distance axially between the terminations⁴.

Mechanical characteristics

The most severe mechanical problem to be solved in the construction of a flexible cable is the tendency for the electrical insulation and conductor tapes to be damaged when the cable is bent on a reel. The problem has received attention for the kraft paper insulation of conventional cables⁷ and the body of knowledge in this subject was extended to plastic film cable insulation during the development of the superconducting power cable⁸.

The problem was exacerbated for the production of the prototype superconducting cables as limitations of the taping machine required 12 separate passes through the taping line during construction⁴. The two cables were made in one continuous length of 300 m. This method

Table 1 Characteristics of the 1000 MVA test system

Number of cables	2
Length of each cable (m)	115
Cable outer diameter (over armour) (cm)	5.84
Inner conductor diameter (cm)	2.95
Enclosure outer diameter (cm)	40
Maximum operating temperature (K)	9
Operating pressure (MPa)	1.55
Cooldown time (h)	100
Rated voltage (3-phase) (kV)	138
Rated impulse withstandability (kV)	650 ^a
Maximum steady state power rating (MVA)	980
Emergency power level (MVA) (1 h) ^b	1430
Surge impedance load (MVA)	872
Surge impedance (Ω)	25
Current-dependent loss at rated power, 3-phase (7.5K) (Wm^{-1})	0.8
Voltage-dependent loss at rated power, 3-phase (7.5 K) (Wm^{-1})	0.15
Enclosure heat in-leak, 3-phase (7.5 K) (Wm^{-1})	0.45

^aMaximum sustained to date is 488 kV

^b1 h is maximum period at 1430 MVA sustained to date

required reeling and unreeling during each pass – a severe test. The cables were installed at the test site by pulling ≈ 150 m, cutting, and then pulling the remaining 150 m of cable so as to provide cables in the cryogenic enclosure lying side by side. A maximum pulling force of ≈ 180 kg was required. After installation the cable was carefully examined. The reeling and unreeling and installation pull had not resulted in mechanical damage to the conductors or electrical insulation.

Electrical performance

The performance of the cables was measured during the eight operating runs from October 1982 to June 1986. These tests included operation under rated conditions, abnormal and emergency ratings, and limited life tests. The first six runs were devoted to 60 Hz electrical measurements, the capability of the cable insulation to withstand impulses was measured during the seventh and eighth runs. The electrical characteristics of the cables are given in Table 1.

Operation under rated conditions. These characteristics include conductor losses, conductor critical current and 60 Hz and impulse performance of the cable insulation.

The most important current-dependent properties are losses and critical current, i.e. the maximum current before quenching. Both these properties are functions of the temperature. In practice the temperature varies along a cooling loop – the design range is 6 K inlet and 8 K outlet – thus the current-dependent properties also vary along the length of the cable.

Loss measurements of both cables were made over the range 250–6000 A, corresponding to 27–648 A cm^{-1} at the surface of the inner conductor. The losses were measured over temperatures of 7–13.2 K. These measurements are not easy to do and inaccuracies no doubt exist in the data given; typically a loss measurement for these cables corresponds to measuring a power factor angle of 125 μrad , a task complicated by the magnetic field present near the terminations where the instrumentation wires emerge. Typically, a field of 20–100 $\times 10^{-4}$ T is present. This field gives rise to induced voltages in the loss measurement instrumentation which is synchronous in

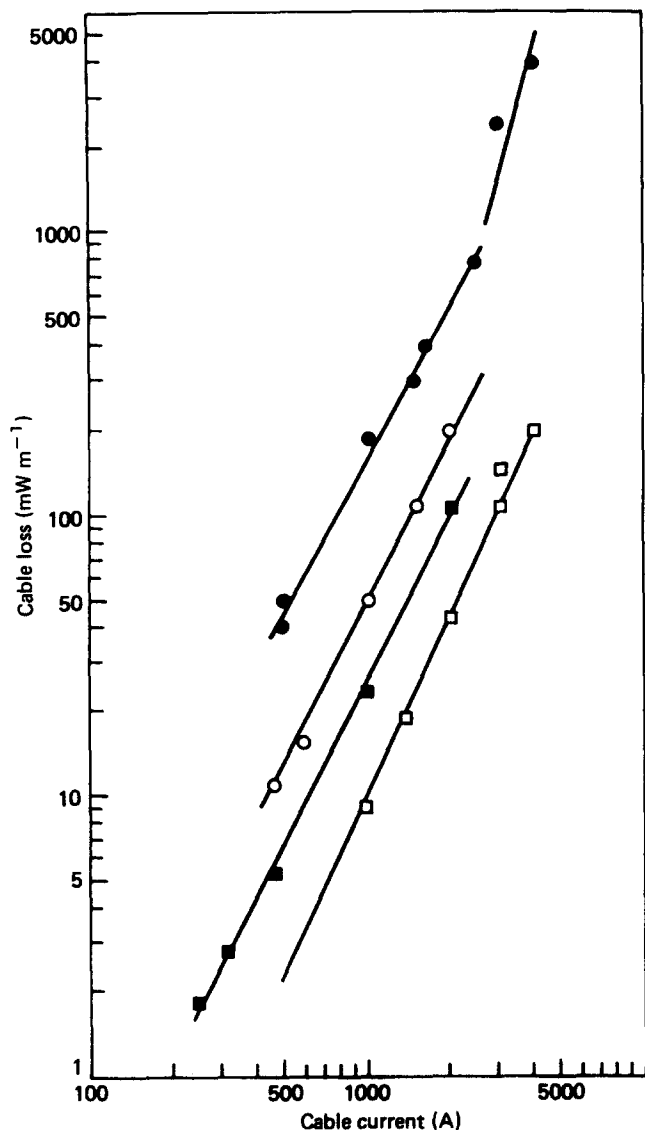


Figure 4 Conductor-dependent loss as a function of cable current (at 60 Hz). ●, 13.2 K; ○, 11.9 K; ■, 11.7 K; □, 9.5 K and below 8 K. The break at the upper end of the curve for 13.2 K corresponds to a quench

frequency with the signal of interest. Errors also exist in the temperature measurements, furthermore, the temperature varies along the cables under test and as a function of time.

The loss per metre of one cable is given in *Figure 4* as a function of line current with temperature as a parameter. The loss is shown for 9.5 K and below 8 K as the lowest curve in *Figure 4*. For example, at the rated current of 4100 A (443 A cm⁻¹) the losses are ≈ 200 mW m⁻¹, this value is consistent with measurements in the laboratory on 10 m cables⁹ and is about a factor of two higher than desirable. One problem in characterizing the current-dependent loss is illustrated by *Figure 5*, which shows how losses vary with temperature at a constant line current of 3000 A (324 A cm⁻¹). This highly non-linear dependence has been observed in laboratory tests¹⁰. The peak centred on 8.9 K is caused by unreacted niobium in the conductor which has a critical temperature of ≈ 9 K. The influence of the niobium on the losses is due to the current paths in the double-helix conductor; in the inner conductor, current circulates from top to bottom of the outer tape, thus crossing the niobium layer. A similar effect occurs in the inner tape of the outer conductor. The experimentally measured points shown in

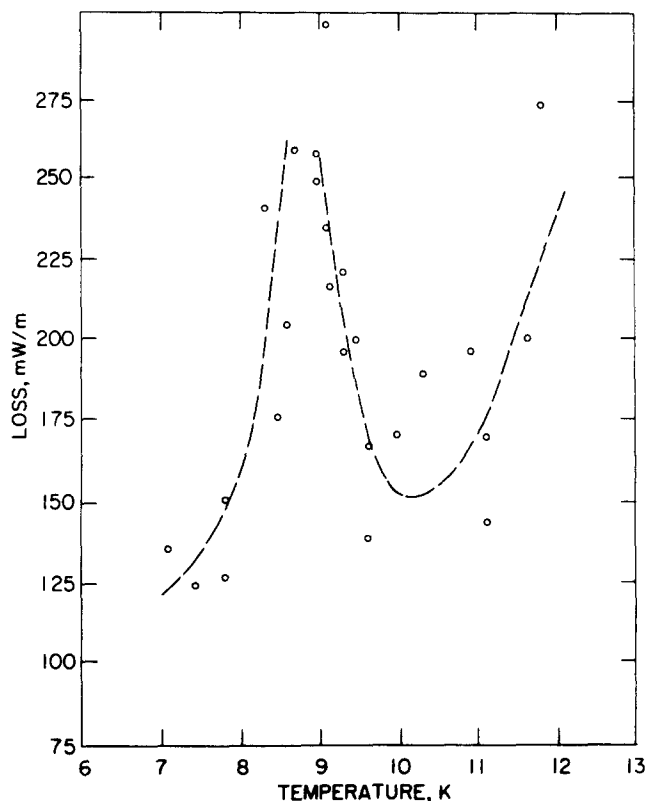


Figure 5 Current-dependent loss as a function for temperature (for 3000 A, 60 Hz). The peak at 9 K is due to unreacted Nb in the superconductor, the operating range of the cable is 6–8 K

Figure 5 illustrate the inevitable scatter present; further measurements may well justify a lower specific loss below 8 K. It was found that the peak losses as a function of temperature could be reduced by the addition of 1% zirconium to the Nb₃Sn alloy¹¹.

The losses vary as the square of the current, a result in line with previous measurements on 10 m long cables⁹. Measurements on small samples and a theory of loss mechanisms produce a higher power for the loss dependence¹² suggesting hysteresis does not contribute to a large component of the total loss; nevertheless, examination of the loss voltage waveform shows a high harmonic content characteristic of hysteretic loss.

The effect on conductor loss of unbalanced inner and outer conductor currents was investigated for differences ≤ 1%. The change in losses was negligible (≈ 1 mW m⁻¹) and it may be assumed that zero sequence components up to several percent will not be a problem.

Even though the losses are somewhat higher than desirable, under normal ratings the current-dependent losses do not predominate, since these losses fall in proportion to the square of the cable current¹³. Consequently, these losses are economically important only during those periods of operation under the worst contingency conditions. Several effects may contribute to the higher than expected losses, the major cause is apparently due to non-linear current distributions near the edges of the tape conductors. This effect increases the losses of both conductors but it is particularly noticeable for the outer conductor, which would otherwise have one-half the losses of the inner due to the 2:1 diameter change. In fact, the losses of the inner and outer conductors are about the same. The crowding of current at conductor edges has been studied for simple helices¹⁴ but not for conductors made with two helices, as in this case. However, it would appear that useful improvement of the conductor losses can be made when the effect has been

analysed and appropriate design changes made to the conductor tape. A thorough analysis of this effect may also explain the square law loss dependence on current mentioned above.

At some time between the second and fifth run the losses of the outer conductor of the north cable increased by ≈ 10 W ($\approx 40\%$) at full rated current. A cryogenic bushing connected to the cable was changed twice during the same period and it seems likely that the cable was slightly damaged during this procedure; a change in resistance of $< 1 \mu\Omega$ would account for the increase. The other conductors functioned without deterioration during all operating runs.

The critical current is the maximum current carried by the cable at a given temperature without quenching. When a quench occurs the current is diverted into the stabilizer layers; a phenomenon investigated closely with 10 m long cable samples¹⁰. To determine the quench current a pulsed power supply must be used to maintain isothermal conditions in the cables. If continuous a.c. excitation is used at these very high current levels, heating will cause a quench after a period of time. The relationship of critical current and temperature is given by

$$I = I_0 (1 - (T/T_c)^2) \quad (1)$$

where I is the maximum supercurrent at temperature T ; T_c is the critical temperature; and I_0 is the maximum current at $T = 0$. A typical value of I_0 for the cables, based on extrapolation of laboratory measurement, is ≈ 30000 A, and for this Nb_3Sn , $T_c \approx 16.6$ K.

Gas-impregnated plastic film is an insulation system which is critically affected by the electric field enhancement in the butt-gaps between adjacent tapes. In a properly made cable, partial discharge in the butt-gaps is the first sign of stress as the voltage is raised. The design of good screens and control of surface irregularities are the attributes of a properly constructed cable. The onset of partial discharge leads to an increase in dielectric loss and, ultimately, failure of the cable insulation. Clearly the limiting factor in the allowable stress imposed on the cable insulation is the intrinsic breakdown characteristics of helium gas under the operating conditions of the transmission system; in this case a minimum helium density of 100 kg m^{-3} .

Figure 6 shows the intrinsic breakdown stress of supercritical helium as a function of density and the onset of partial discharge activity in various cables. The top curve shows breakdown characteristics for helium between closely-spaced metal gaps. It can be seen that the curve varies from the ideal Paschen's Law¹⁵, which predicts a linear relationship between stress and density for fixed gaps. Curve c (Figure 6) represents the best laboratory short samples and was measured during the development phase using a 1 m sample wound on a smooth metal mandrel¹⁶. This model was made with 50/50% butt-gap registration; a design which ensures that the ratio of partial discharge inception stress across the inner gap to the stress across the total insulation thickness is less than the ratio for any other registration distribution. The limiting performance for the insulation is when the maximum stress on a butt-gap (usually the innermost gap) approaches Meats' curve¹⁶.

The onset of partial discharge activity in the cables is shown in curve d (Figure 6); no data is known for densities $> 43 \text{ kg m}^{-3}$ because the excitation equipment is not rated for voltages > 110 kV and no partial discharge above the background is observed below this voltage for

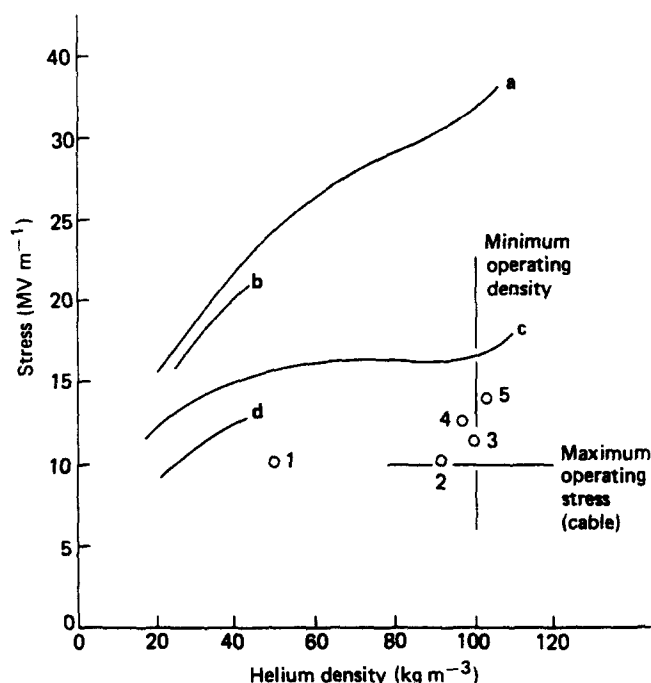


Figure 6 Partial discharge inception stress as a function of helium density. \circ , Conditions without partial discharge activity: 1, rated voltage with the conductor quenched; 2-5, endurance tests during the second run. a, 0.125 mm metal gaps (Meats); b, inner butt-gap of cable; c, best laboratory short sample; d, cable inner conductor.

densities $> 43 \text{ kg m}^{-3}$. The radial distribution of butt-gaps can be determined, and the radial distribution of voltage calculated based on the cable construction.

Such a calculation leads to curve b, the inner butt-gap of the cable. This curve is close to Meats' results for small gaps and thus the cable almost reaches a partial discharge stress set by the intrinsic performance of helium. The ratio of stress across the innermost gap to average stress across the cable insulation is a designer's choice and depends on the registration of butt-gaps. Although 50/50% registration yields good 60 Hz performance it is thought that the ability to withstand impulse is reduced because of the shorter path for 'zig-zag' breakdown. The resolution of partial discharge activity is ≈ 0.5 pC for small samples and ≈ 100 pC at the cable test facility. The circles correspond to various operating conditions where partial discharge was not observed. For example in Figure 6 circle 1 is the operating point for the insulation when a rated voltage of 80 kV 1-n was applied during a quench at full current (4100 A) caused by operating above the critical temperature (T_c). Circle 5 corresponds to conditions during the 13 h endurance test in the second run when 110 kV was applied. It would appear that there is at least a margin of 50% between the operating point at maximum voltage and minimum density and the possible onset of partial discharge activity. This margin is similar to those observed in samples subjected to accelerated life tests and in which lifetimes > 30 years could be extrapolated for operation at an average stress of 10 MV m^{-1} .

The dielectric loss of the cable cannot be measured electrically as the full current outer conductor prevents a separate connection to the screen necessary for a three-terminal bridge connection. During the 110 kV endurance test an attempt was made to measure losses calorimetrically but this is a difficult technique due to dissipation in the bushings and the fact that the system was not stabilized thermally at the time. The test indicates a maximum thermal increase from all sources of 13 W per cable or $\approx 110 \text{ mW m}^{-1}$. Assuming the loss factor is not stress

dependent this scales to 60 mW m^{-1} at 80 kV 1-n. This loss is not significant for a 138 kV system but becomes more onerous at higher voltages. The polypropylene laminate used in the cables is more lossy than desirable. It has a laboratory measured short-sample dissipation factor of $25 \mu\text{rad}$, probably due to the glue bonding the layers. The north cable has been impulsed up to 488 kV during the eighth run. At this level the stress cone on the west end of the cable failed. A.c. tests performed after the impulse test indicate the cable is undamaged.

Abnormal and emergency conditions

The cables were operated at full current in a quenched condition during a cool-down. In Figure 4 it can be seen that there is a distinct increase in the slope of the loss curve above 2500 A at a temperature of 13.2 K. This corresponds to a quench in the cables, but as the current was continuous there is no doubt that local heating drove portions of the cable above the average of 13.2 K. The importance of the critical current level is related to the ability of the cable to carry three-phase faults without damage.

The emergency rating of the superconducting cables is a transmission power level above the maximum continuous contingency thermal rating of the cables but below the maximum current for cryostability. For this system the emergency rating was specified initially (somewhat arbitrarily) as 6000 A for 30 min which is 46% over the steady state thermally-limited current of 4100 A. During the second and third runs, this test caused the cryogenic bushing of one termination to crack at the warm end; current was indeed carried for 30 min but when voltage was applied the cracks caused a breakdown of the bushing insulation (see below).

During the sixth run the current was raised to 5 kA and the rated voltage of 80 kV to ground was applied. After lead-flow adjustment, the current was raised to 6000 A. There were no electrical or thermal problems observed in the specified 30 min period. After that the voltage was raised to 110 kV to ground. The voltage and current levels were returned to 80 kV and 4100 A, respectively, after 1 h at 6000 A. For 20 min the cables were carrying 660 MVA per phase. Based on the temperature rise during this test, shown in Figure 7, it would appear that 6000 A could be carried for several hours, but cryostability after this period will have to be verified experimentally. Figure 7 illustrates an interesting phenomenon observed on many tests of the system – frequently an increase in heat load initially produces a

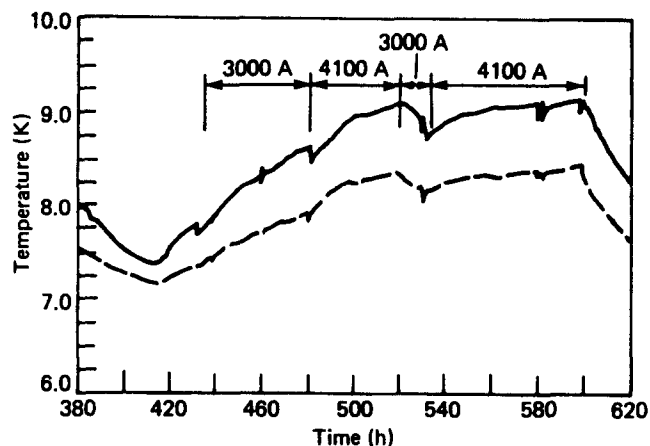


Figure 8 Temperature variations during the life test.—, High power 'go'; ---, low power 'return'

decrease in temperature at some locations. This behaviour, typical of functions with non-positive real characteristics, is caused by expanded warm gas in the load driving an increased flow of cold gas into the refrigerator.

It is also desirable to have the system to continue to function after a refrigeration failure. Such a capability is possible in a superconducting system because of the very large heat capacity of the helium in the cryogenic enclosure. (There is $\approx 5 \text{ kg}$ of helium per metre of length at an operating temperature of 7.2 K.) As the system slowly warms, the helium expands and must be allowed to exit the system if the maximum operating pressure of the vessels is not to be exceeded. Most of the heat enters the system at the terminations. By allowing the expanding helium to exit the system through heat exchangers located in the terminations, the entire system can be kept in the operating temperature range. Using these techniques, the cables have operated at full current and voltage for $> 100 \text{ min}$ after refrigerator shutdown. Considerably longer times should be possible in larger systems, as would be the case in an actual installation.

Life tests

The longest run during the testing sequence was 27 days. The first five days of each run are spent cooling the system to its operating temperature of 7–8 K. During the sixth run, the cables were operated at current levels of 3000 A and above for ≈ 10 days. Both voltage and current were applied for nearly 75% of that time¹³. Figure 8 shows the temperature change with time after power is applied. The temperature increase is principally due to the increased helium flow required at the terminations; the total flow per termination increases from 0.125 to 0.395 g s^{-1} .

In addition, as the operating runs became longer, it became more difficult to staff the site for 24 h operation. The system is self-regulating and as the number of automatically monitored functions increased, the burden for the operators decreased once the system had reached operating temperature. Therefore, the computer was given the ability to access the public telephone network and deliver a voice-synthesized message should an alarm condition arise. As a back-up, an entirely separate, battery operated, automatic dialing alarm system was also installed. It informs the operators on its call-down list when a loss of electrical power occurs. The computer control system is described below under the section 'System monitoring and data acquisition'. With this system in place, the test site has been operated with only one staffed 8 h shift per day after the system has reached

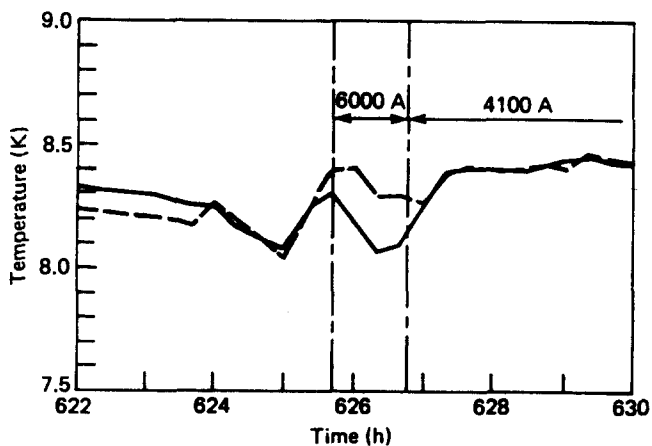


Figure 7 Temperature variations during the emergency rating test for the south cable.—, West; ---, east

Table 2 Summary of operating runs and life tests

Number of operating runs	8
Total time cold (h) ^a	2727
60 Hz electrical tests	
Voltage and current at 240 MVA/cable (h)	89
Voltage and current at 330 MVA/cable (h)	166
Total time with voltage or current (h)	441
Emergency rating of 6 kA and 80 kV 1-n (480 MVA/cable) (h)	1
Maximum power test, 6 kA and 110 kV 1-n (660 MVA/cable) (mins)	20
Overvoltage at 90 kV 1-n (h)	22
Overvoltage at 100 kV 1-n (h)	19
Overvoltage at 110 kV 1-n (h)	13

^aIncludes cooldown at start of each run (≈ 100 h for the first seven runs and ≈ 76 h for the eighth run)

operating temperature. Even the use of a single shift is mostly the result of the need to perform short term experiments on the superconducting cables or cryogenic system, and on weekends a full 8 h shift is dispensed with. A summary of the limited life testing is given in *Table 2*.

Terminations

A three-phase superconducting power line would require six terminations. The test facility uses only four, one at each end of the two cables, but their design is appropriate for use in an actual utility installation. An exploded view of a termination is shown in *Figure 9*. The termination design may be divided up into three major portions. The first part provides the anchor point for the cable armour and allows the outer conductor to be attached to a large copper cylinder which carries the outer conductor current. Inside the cylinder the cable insulation is formed into a

stress cone to grade the horizontal component of the electric field so that the inner conductor is exposed. A perforated joint is made to the inner conductor so that coolant gas can be forced down the inner core of the cable. In the second region the inner and outer conductors are joined to a device known as the cryogenic bushing. This is a coaxial current-carrying bushing which is cooled by gas. By correct choice of the heat transfer rate and gas flow a temperature gradient is formed along the cryogenic bushing between ambient temperature and the operating temperature of the cable, both parts are cryogenic and need an insulating vacuum space around them. In the Brookhaven design both these regions are horizontal, mainly for ease of assembly. The third portion is a large, but fairly conventional, air entrance bushing which is vertical. The insulating medium is SF₆ gas. The temperature of the joint region at the ambient end of the cryogenic bushing and the SF₆ elbow is stabilized by a water/glycol mixture fed from a pump at the top of the elbow. The water/glycol mixture circulates in a heat exchanger inside the centre conductor of the cryogenic bushing and absorbs the heat generated there when high a.c. currents are flowing in the aluminium conductor. When no current is present, this heat exchanger, along with another water/glycol loop which is welded to the flange connecting to the outer conductor of the bushing, serve to keep the temperature of the ambient end of the bushing from falling too low. A view of the two air-entrance bushings at the east end of the test facility is shown in *Figure 2*.

The cryogenic bushing required extensive development over a period of several years. The bushing must carry 4100 A on its inner and outer conductors, electrically insulate these two conductors from each other, incorporate heat exchangers to intercept the I^2R heat as well as the heat transported by thermal conduction from its warm end, and withstand the mechanical stresses introduced by a temperature differential of 290 K. These requirements

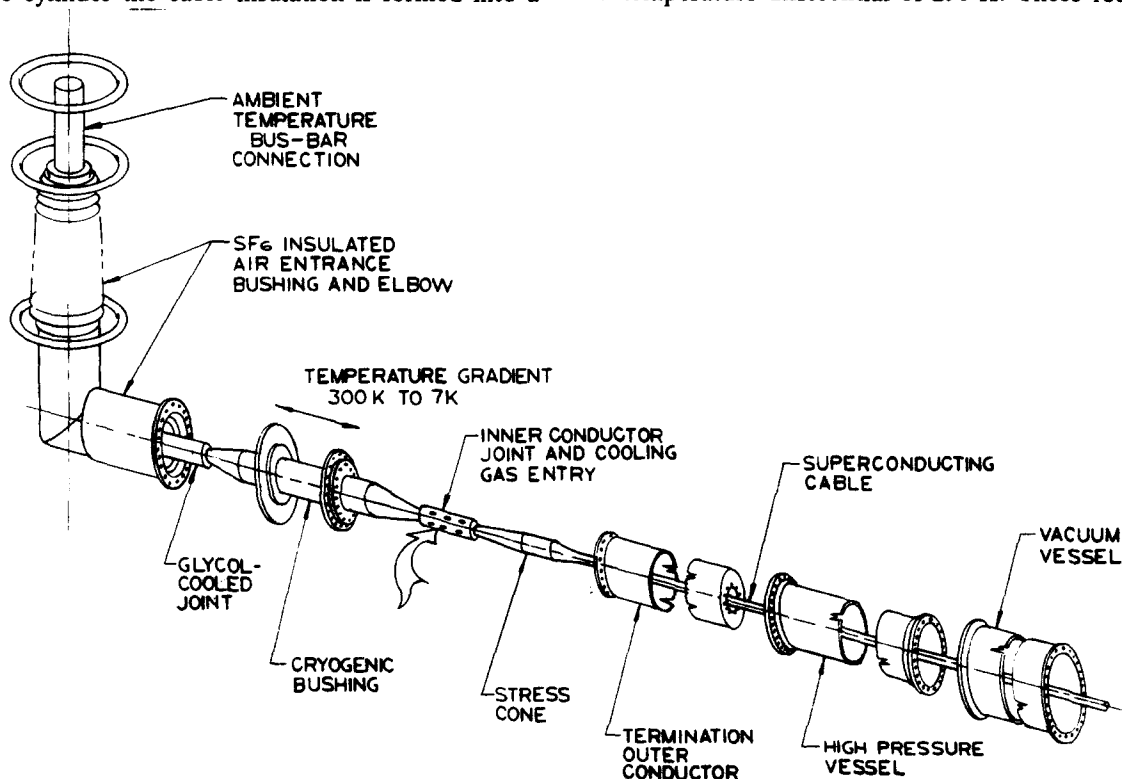


Figure 9 Termination for a superconducting cable. The cryogenic portion of the termination is horizontal. The cable end is on the right, the inner conductor is exposed by terminating the dielectric insulation with a hand-built stress cone. Both inner and outer conductors are attached to the cryogenic bushing which makes the connection across the temperature difference of 300 K between the cables and the ambient temperature busbars. The ambient temperature portion is an SF₆-filled elbow which is vertical. A pump at the top of the air-entrance bushing circulates a water/glycol mixture to cool the inner conductor of the elbow

presented a technical difficulty equal to that of the development of the superconducting cables themselves. Originally the bushing was made with loaded epoxy, a method that permitted the thermal construction of the insulating material to match the conductors¹⁷. Unfortunately, large epoxy castings are difficult to make without retaining high internal stresses produced during cool-down after curing. Thus bushings made this way are prone to cracking when additional differential mechanical stresses are imposed during cool-down of the cryogenic system. In the end, the bushings used in the four terminations at the test site were made of epoxy impregnated paper rolls with built-in capacitive grading¹⁸.

The temperature gradient on the colder portion of the bushing is maintained by a small flow of cold helium gas ($\approx 0.4 \text{ g s}^{-1}$ total for each bushing at 4.1 kA). The gas flows through helically wound tubes on the inner and outer conductors. The warmer portion has a water/glycol cooling system. The helium flow is regulated so as to maintain the desired temperature at the cold end. This flow must be varied as the current being carried by the cable varies.

At the operating current of 4100 A the resistive loss in each cryogenic bushing is $\approx 800 \text{ W}$. Only $\approx 60\%$ of this additional heat load must be absorbed by an increased helium flow, however, since the water/glycol heat exchanger efficiently removes heat generated at the bushing's warm end. Each conductor of the bushing was originally designed to have a resistance of $20 \mu\Omega$, but fabrication difficulties resulted in the final production bushings having conductor resistances of $40 \mu\Omega$ and outer conductor resistances of $10 \mu\Omega$. Consequently, the conductive heat flow is twice as large as originally planned for the outer conductors, but the resistive heating is halved, and conversely for the inner conductors.

As the heat that leaks in through the cryogenic enclosure for the cables is so small per unit of length, most of the heat load for relatively short systems occurs at the ends. About 180 W attempts to flow by conduction through the cryogenic bushings themselves and is mostly absorbed by the helium flowing out through the heat exchangers on the aluminium conductors. Another 160 W does reach the cryogenic region by conductive and radiative heat transfer through other parts of the system, particularly by radiation on the large pressure vessels, which have an area of 4.17 m^2 each, and by conduction at

the valves, which have stems that extend to ambient temperature positioners, see Figure 10. During normal operation, cold helium gas from the refrigerator first flows through a heat exchanger spirally wound on the pressure vessel before it enters the system.

During the eight operating runs several failures of termination components occurred. During the first run the start of cooling gas flow to the termination conductor produced a thermal shock in the small insulators used to float the helium plumbing of the outer conductor off ground potential; the subsequent small helium leaks then caused the vacuum pressure of two terminations to rise to an unacceptable level. The insulators were re-designed for subsequent runs and, in addition, the cool down procedure was amended so that termination cooling occurred when the third and fourth turbines were started (see 'Cryogenic system' section below) at $\approx 100 \text{ K}$. During the second and third runs the system was operated at the emergency rating of 6000 A; on each occasion the conductor expansion at the warm end of the bushing caused the insulation to crack in that region. The cracking was detected by applying voltage during the current test. The failure occurred in the same termination on each run. An investigation showed that an accumulation of tolerances had greatly increased the axial pre-stress on the bushing during assembly compared to the other three terminations. On the sixth run, with a new bushing installed, the emergency rating test of 6000 A for 30 min was accomplished without difficulty. The voltage was then raised in 10 kV steps to 110 kV to ground for $\approx 20 \text{ min}$. If any cracks were developing in the bushing they would have been detected in this test but no ill effects were observed.

Before the seventh run the system was reconfigured. The north cable was separated from the 60 Hz excitation equipment and connected to a five-stage Marx generator at the west end. Extensive changes were made to the grounding system (see 'Electrical excitation system' section below). A terminating impedance was connected at the east end to produce the proper waveform for an impulse test – a unidirectional voltage waveform with a $1.5 \mu\text{s}$ rise time and $50 \mu\text{s}$ fall to half peak value. After the cable system had withstood several positive and negative impulses at 150 kV, the cryogenic bushing at the east termination failed on the first shot at the 340 kV peak level due to an insulation failure at the warm end. There

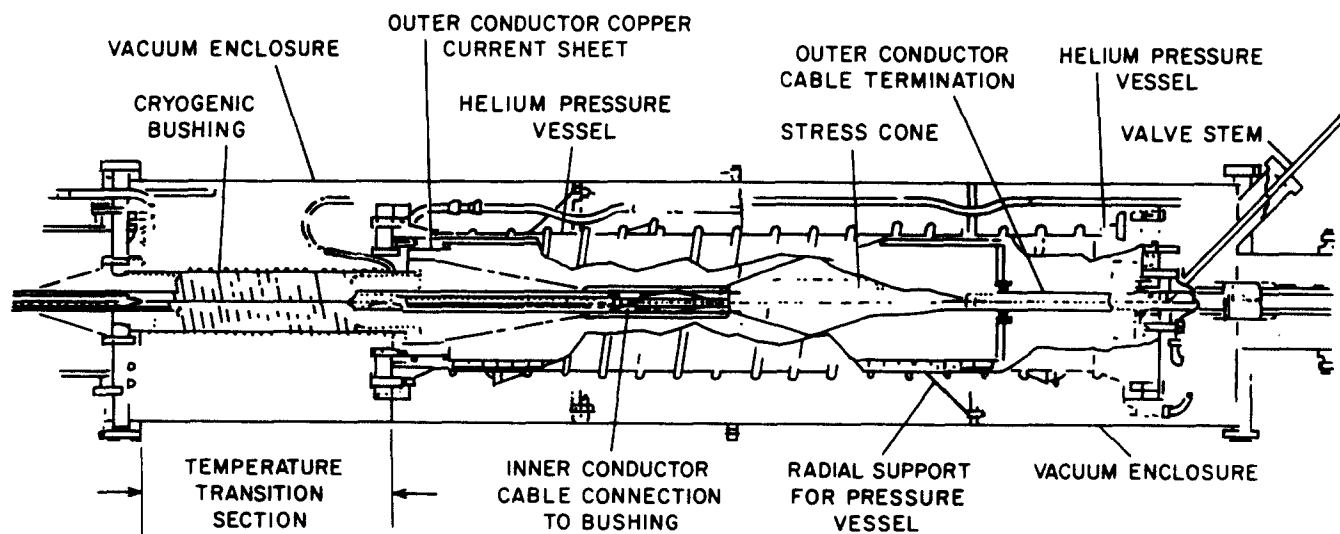


Figure 10 Layout of a termination showing major cryogenic components. The room temperature elbow, which is not shown, connects to the warm end of the cryogenic bushing at the left of the assembly

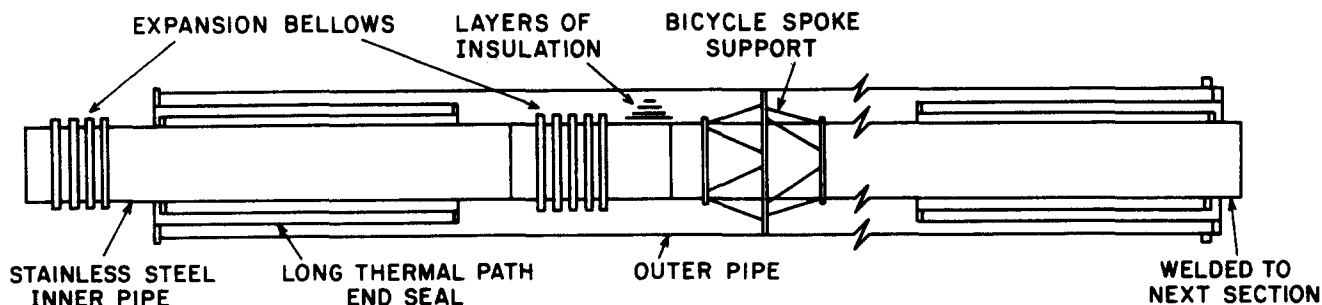


Figure 11 Design of the cryogenic enclosure. The re-entrant seals at each end permit a permanent vacuum space within the annulus of the enclosure

was evidence of poor impregnation of the paper roll at the failure point.

The bushing was replaced before the eighth run. At peak impulse level of ≈ 500 kV (negative polarity) a failure occurred in the hand-applied stress cone at the west end of the cable. Rated 60 Hz voltage was applied after the impulse test and the cable itself does not appear to be damaged.

Cryogenic enclosure

The evolution of the cryogenic enclosure is closely tied to the system studies carried out in cooperation with electric utility companies on the potential applications of superconducting power transmission. The first study, performed with the Long Island Lighting Company, revealed that the enclosure design was far too expensive¹⁹. An analysis of the cost after the study indicated two design aspects which contributed significantly to the cost: the use of an intermediate temperature shield; and, one-way cooling with the coolant return piping in the evacuated annulus.

The design was subsequently modified to eliminate the heat shield and to use counterflow cooling^{20,21}. The optimum choice of the heat in-leak load compared to the electrical losses depends on the cost of energy and the cost of money. In the Brookhaven studies the cost optimization was based on reducing capital cost with operating costs set somewhat above the minimum theoretically possible. Systems with the heat load of the enclosure designed to be $\approx 50\%$ of the maximum thermal load give good economic comparisons with other forms of underground transmission²².

After several years of laboratory development²³, the enclosure used at the test site was made available commercially. The 100 m cryogenic enclosure is made up of five sections with welded joints between them. Six sections were manufactured, one is a spare*. A flexible section was obtained later†, but was never installed. The rigid sections are a pipe-within-a-pipe design with welded ends as shown in *Figure 11*. The outer pipe has an outside diameter of 406 mm, while the low temperature pipe has a bore of 213.5 mm; this is more than enough for the two cables in it. The inner pipe is wrapped with multilayer, aluminized plastic sheets to minimize radiative heat transfer, and it is held concentrically inside the outer pipe by spoke-type supports under tension. At the ends of each section, the two pipes are welded together, creating an annulus which is evacuated and sealed only once, at the time of manufacture. The vacuum spaces have not been pumped in the more than eight years since the enclosures were made, and yet they have maintained entirely

acceptable vacuums. Moreover, the rate of increase of the pressure in the vacuum spaces has fallen off with time, stabilizing at ≈ 100 $\mu\text{m Hg}$, as can be seen in *Figure 12*. This vacuum is good enough to permit cooldown to begin. Then, any gases in the annulus condense on the inner pipe by cryo-pumping, and the vacuum becomes essentially perfect. The realization of an enclosure design with these characteristics was a major success of the project.

Cryogenic enclosure performance

During low temperature operation, the temperatures and pressures throughout the system have been recorded. This information allows the thermal heat leak of the cryogenic enclosure to be calculated. Unfortunately, the helium in the inner pipe is at a pressure and temperature where its enthalpy is a strong function of temperature, i.e. the operating point is near the transposed critical line, so the uncertainty in the result is large. From a graphical analysis of ≈ 90 points, the heat leak was found to be no more than 0.45 W m^{-1} . However, the random error in the experimental result is $\approx \pm 0.12 \text{ W m}^{-1}$. Furthermore, small systematic errors in the calibration or accuracy of the temperature sensors or pressure transducers would produce relatively large errors in the result. The heat leak of the enclosure improves with time during a run; this is shown in *Figure 13*.

Cryogenic system

The superconducting cables are maintained at their operating temperature of 7–8 K by a cryogenic system that consists of the following main components:

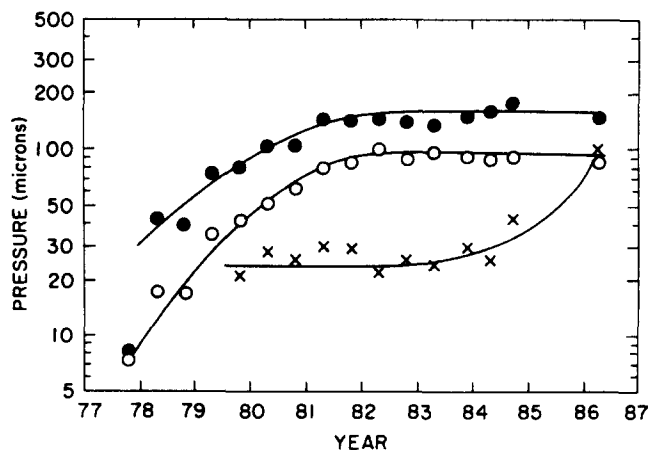


Figure 12 Pressure versus time curves showing a history of vacuum pressure in the cryogenic enclosures measured with the system warm. ●, Spare section (MVE); ○, five installed sections; x, Kabelmetal section. The flexible Kabelmetal section, which is not installed in the system, appears to have developed a small leak in 1985. None of these enclosures have been pumped since manufacture

* These rigid enclosures were made by the Minnesota Valley Engineering Company, USA

† Made by Kabelmetal, Hannover, FRG

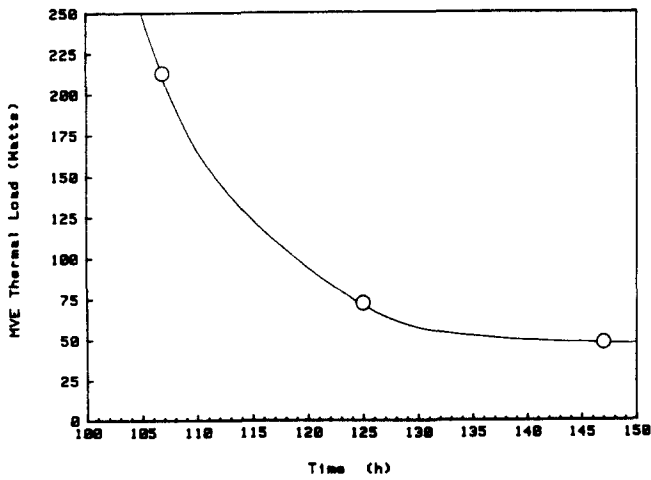


Figure 13 Enclosure heat load versus time showing the measured value of the heat leak into the cable enclosure during the third run. Note that the rate stabilizes after ≈ 140 h from the start of cooldown

- 1 compressor;
- 2 refrigerator cold box and turbine expanders;
- 3 transfer lines;
- 4 cryogenic bushings;
- 5 cable enclosure; and
- 6 control and monitoring system.

In addition, a large number of pieces of supporting equipment are also required. These include control valves, mechanical pumps, vacuum systems, air compressors and driers, a water chiller, helium storage systems, filters, after-coolers, cyclone separators, demisters, charcoal absorber beds, water pumps, laser aerosol detectors, measuring instruments, display monitors, other computer peripherals, and pressure, temperature and flow transducers. Figure 14 shows some of the major components of the system.

The main component of the cryogenic system is a supercritical helium refrigerator with a remote expander. The refrigerator consists of counter-flow heat exchangers and four high-speed gas-bearing turbines which operate in a combined Claude-Brayton cycle. The temperature-enthalpy, T - S , diagram for the cycle is shown in Figure 15. Helium is supplied to the refrigerator at 15.3 atm* pressure by an oil-injected screw compressor. The details of the cryogenic system are different from those of a system that would be designed for a commercial application, but the choice of particular elements of the system

* 1 atm \approx 101 kPa

was constrained by the objective of using equipment that was highly reliable, simple to maintain, and capable of automatic operation^{24,25}.

The single-stage rotary compressor is cooled by the injection of oil directly into the process stream. It is then necessary that all the oil be removed by the demisters and filters before it reaches the heat exchangers of the refrigerator. Therefore, the flow of helium is continuously monitored by two laser aerosol detectors²⁶ to ensure that all particulate matter and oil droplets have been removed. The detectors can detect particles of 0.3 - 3 μm in diameter down to levels of concentration as small as 5 ppb (parts per billion) by weight. The compressor inlet pressure is 3 atm and it delivers $> 130 \text{ g s}^{-1}$ of helium at 15 atm to the refrigerator. The compressor motor requires 320 kW, and the isothermal efficiency is $\approx 42\%$ of that of an ideal helium compressor. Two-stage screw compressors, which have been put into operation subsequent to the completion of the BNL superconducting cable test facility, have exhibited higher efficiencies, $\approx 57\%$.

In the refrigerator, 59 g s^{-1} of the helium flow is diverted. The temperature of this stream is reduced by having it drive two turbine expanders (numbers 1 and 2) in series. It is then used to cool the heat exchangers of the refrigerator cold box. The remaining 71 g s^{-1} passes through the heat exchangers and is delivered to the load at a pressure of 15 atm and a temperature $\approx 7.8 \text{ K}$. After travelling down the centre of the superconducting cables, this high pressure stream undergoes an expansion at the far-end (via the third turbine) and returns outside the cables, but in thermal contact with them, at 7 atm, as shown in Figure 16. Thus, the cables themselves act as counterflow heat exchangers and are cooled by both inner and outer helium flows. The return flow is further expanded by the fourth turbine within the refrigerator cold-box to a pressure of $\approx 3 \text{ atm}$.

System performance

Without lead flow, the main refrigerator can produce $\approx 800 \text{ W}$ of refrigeration at the operating temperature (including $\approx 140 \text{ W}$ resulting from the far-end turbine expander). Since the compressor power is 320 kW, this gives 400 W/W for the ratio of power input to cooling output. In actuality, some of the high pressure helium flow is removed at low temperatures to cool the cryogenic bushings. Once this lead flow exits the heat exchangers on the inner and outer conductors of the cryogenic bushings, it is returned as warm helium gas to the compressor. Consequently, the counterflow heat exchangers in the

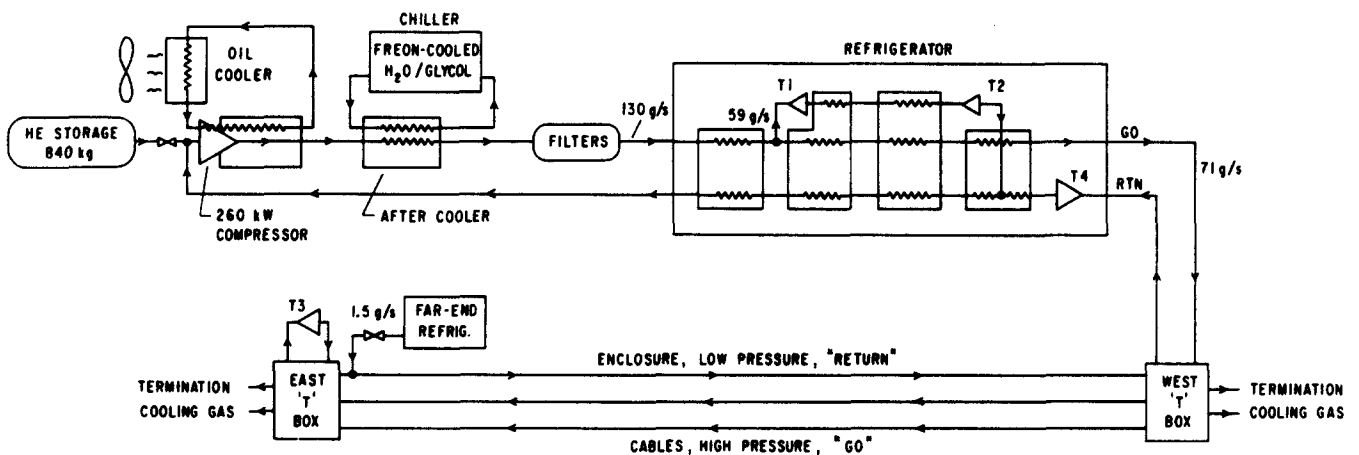


Figure 14 Simplified diagram of the cryogenic system

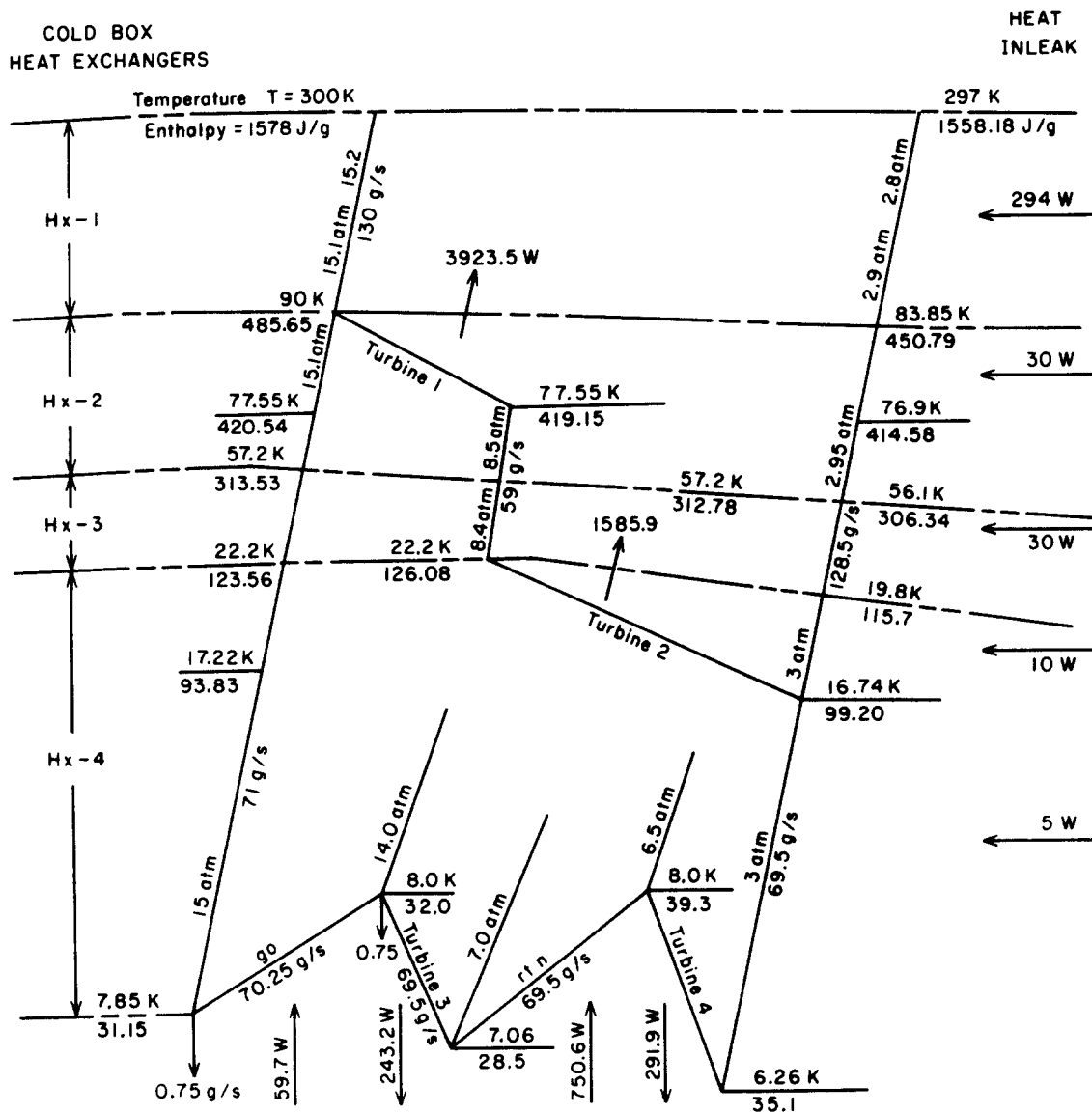


Figure 15 Temperature-enthalpy (T - S) diagram for the main refrigerator

refrigerator cold box must operate with an imbalance in flow, with less cold helium returning than must be cooled and delivered to the load. As a result, there is a loss of refrigeration capacity at the design temperature. A typical value for the loss in refrigeration capacity is $80 \text{ W per g s}^{-1}$ of helium that is returned as warm gas to the compressor²⁷. Actual measurements on the Brookhaven system indicate that it is rather more sensitive to unbalanced flow. The sensitivity as obtained by measurement was $130 \text{ W per g s}^{-1}$ with just 1.3% warm gas recovery. When the cables are unpowered, the small lead flow required to intercept the heat in-leak results in a reduction in capacity to $\approx 670 \text{ W}$, but when the I^2R losses must also be absorbed, a flow of 1.56 g s^{-1} is required and the resulting refrigeration capacity is inadequate for keeping the system in the designed operating range. To compen-

sate for this loss, a supplemental refrigerator was added during the later stages of construction which supplies $\approx 1.5 \text{ g s}^{-1}$ at 7 K and thus compensates for the unbalance introduced by lead flow.

The main refrigerator is equally sensitive to unbalanced heat exchanger flows of the opposite sense. When heating occurs in the load, the resulting expansion of the helium there causes less helium to be accepted from the refrigerator, but the returning flow does not decrease. This condition results in overcooling of the high pressure helium stream. This stream is also the source of the helium going to the upper-stage turbines. The rapid cooling of this stream as it moves through the heat exchangers results in equally dramatic pressure drops. These pressure drops can cause serious problems in the operation of the gas-bearing turbines. However, now that these difficulties have been experienced, it is easy to conceive of design changes that would ameliorate these effects.

A heat balance is shown in Table 3. It can be seen that the 'go' transfer line was gaining a significant amount of heat. In addition the W2 termination suffered from poor seals which were intended to prevent helium convection circulation¹⁸. When the bushing was replaced in 1984 this extra heat load was eliminated. In late 1985 the cold-box was moved to a location which was much closer to the west terminations. This change greatly

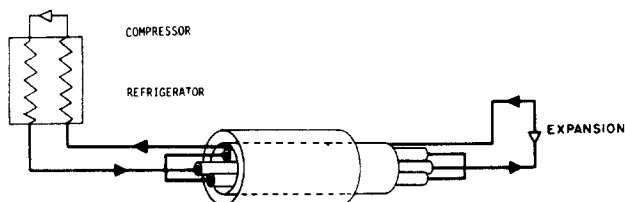


Figure 16 A method of reducing cost by forming a counterflow heat exchanger from the cable and the enclosure

Table 3 System heat balance (prior to 1984) (conditions: far-end refrigerator not running; no electrical excitation)

Heat load	
'Go' transfer line (W)	109
'Return' transfer line (W)	30
Cryogenic enclosure (W)	50
Termination W1 ^a (W)	234
Termination W2 (W)	442
Termination E1 (W)	263
Termination E2 (W)	215
Total (including lead flow)	1343
Lead flow cooling	
Termination W1	146 W at 0.10 g s ⁻¹
Termination W2	246 W at 0.177 g s ⁻¹
Termination E1	141 W at 0.10 g s ⁻¹
Termination E2	143 W at 0.10 g s ⁻¹
Total	675 W at 0.477 g s ⁻¹
Refrigeration	
Main refrigerator (W)	526
Far-end expander turbine (W)	142
Total	688 W + 0.477 g s ⁻¹

^aTermination loads include all losses associated with the ends

reduced the heat load of the 'go' and 'return' transfer lines. The calculations shown in *Table 3* are subject to considerable uncertainty due to the sensitivity of the measurements to errors in deriving temperature differences.

During the eighth run, performed in 1986, it was found the reduction of the heat load resulting from the changes to the refrigerator decreased the cooldown time by ≈ 24 h compared to the earlier runs.

The turbines themselves have operated reliably. Each has dynamic gas bearings and a closed-cycle brake compressor which gets its gas from the process stream²⁸. Initially, turbine failures occurred as a result of an apparent improperly designed seal in the turbine housing. This seal was essential to keep the water/glycol coolant for the brake circuit from leaking into the process helium stream.

After re-design two failures occurred. One was due to the necessity of overriding the automatic protection system to perform a test at the end of the fourth experimental run. The test was to determine the rate of temperature rise in the cable enclosure after a loss of refrigeration. At the time the cryogenic system was designed, it had not been foreseen that one would want to power the cables with the refrigerator shutdown, and, in fact, the automatic valve configuration system made it impossible to maintain the helium in the cables at design pressures when the refrigerator was not running. Therefore, it was necessary to override the automatic protection system and perform an abnormal manual shut-down. As it turned out, a pneumatic valve controller when manually operated, could not close the turbine number 1 inlet valve rapidly enough to prevent its overspeeding and subsequent self-destruction. Changes were later made to the system to allow this test to be performed with all automatic controls enabled.

The second failure occurred during the sixth experimental run and involved the far-end turbine, turbine number 3. It was planned to re-start the refrigerator at the end of the run, 1 h after having shut down the system. The third turbine had always been reluctant to start, and would not start on this occasion despite many attempts. It was apparently damaged. The replacement turbine performed well in the seventh run, and, in fact, was easily started

even when cold on two occasions. (These two cold re-starts were necessitated by the loss of electrical power from the local utility during thunderstorms.) It was noticed that the turbine that was replaced was always more difficult to rotate by hand than the others, including its replacement, and it may have had an unusually tight-fitting plastic insulating pad.

The helium system itself, including storage tanks, compressor, refrigerator, and load, is a closed system in which the helium is continuously circulated. It is essential that this large system be helium leak-tight since even a small leak will result in a significant loss of helium over time. The helium inventory for the test facility is 875 kg, ≈ 520 of which are in the load at operating temperature. Some of the runs lasted as long as 27 days, so even a leak rate as small as 0.04 g s⁻¹ would result in a loss $\approx 10\%$ of helium during the run.

Leaks did develop in the system over time, one in a cryogenic bushing connection and another in piping flanges for a helium filter. So that such leaks might be detected and corrected as early as possible, instrumentation was added to measure the pressure and temperature of the helium in all the large volumes of the system, including storage and buffer tanks. Then the program of the computer monitoring system was modified so that the total mass of helium was regularly calculated and compared to the amount in the tanks at the beginning of the run.

System monitoring and data acquisition

Operation of the cooling plant would be impossible without the computer-based data acquisition, analysis and control system²⁹. The data acquisition system is controlled by a commercial 'personal technical' desktop computer with hardware and software optimized for instrument control over the IEEE-488 bus. It uses a MC 68000 8 MHz 16/32-bit processor, but also contains three other LSI processors and controllers to free the MC 68000 for intense computational tasks. It is programmed in a structured, high-level, interpreted language with extensions for instrument control and real-time processing.

The program itself is 'interrupt driven', that is, the section of the program that is executed next is determined by what happens in the real environment as communicated to the computer by instruments, transducers, or the time as given by an internal clock. The information collected and interpreted by the computer is displayed pictorially on a pair of colour monitors. These displays are colour-coded for easy interpretation by the operators. Values that are out of the expected range are flashed and a warning message is also delivered by a voice synthesizer. Plots of temperature *versus* time are also available on the display.

About 100 transducers are monitored throughout the system, many of them in inaccessible places such as the low-temperature cable enclosure or the top of a high-voltage bushing. The quantities monitored by the data acquisition system are given in *Table 4*.

Alarm conditions, possible malfunctions and system status are also monitored by the computer system. The alarm conditions are of two types:

- 1 alarm conditions determined by measurement and calculation from information supplied by the regularly sampled pressure, differential pressure, temperature, or vacuum transducers; and
- 2 alarm conditions signalled by the opening or closing of a relay in the hard-wired alarm and status circuits of the facility. A few of the most critical of the latter are

Table 4 Computer monitored quantities

Quantity measured	Type	Number
Pressures		
Absolute	Capacitive	23
Difference (flow)	Capacitive	4
Difference (flow)	Pneumatic & P/E	1
Temperatures		
< 55 K	Germanium	42
> 55 K	Platinum	34
other, < 270 K	Type J tc	7
Vacuum pressures		
< 0.1 Pa	Ionization gauge	4

connected to an event-sense card. These are listed in Table 5.

Since the system is self-regulating and automatically monitored, once the system has reached operating temperature little or no operator attention is required. In fact, the site is not staffed for 16 h of the day during this period of the run, even when there is full power on the cables. When human intervention is required, the computer telephones standby operators and delivers a voice-synthesized message. During normal operation, it answers incoming calls with a summary of the status of the system.

For high reliability, all critical alarms are hard-wired; i.e. the signals from the transducers detecting the alarm condition directly control solenoids and valves that will put the system in a safe configuration. The computer merely monitors the presence or absence of these alarm signals and alerts those individuals on its call-down list.

There are some alarm situations which can be detected only through computation and comparison with previous results by the computer. In these cases, the computer itself can turn off equipment to protect the system. Of course, loss of electrical power to the site immediately results in a safe shut-down. The computer monitoring system automatically restarts upon restoration of power.

As an added back-up, a battery-operated automatic

Table 5 Events and alarms

Number	Situation
1	Main refrigerator compressor not running
2	Power dip, no a.c. power, or missed a.c. power cycle
3	Far-end lead-flow refrigerator compressor not running
4	Pneumatic instrument air, vacuum, or a.c. power failure at east end of superconducting cables
5	Pneumatic instrument air, vacuum, or a.c. power failure at west end of superconducting cables
6	Main refrigerator turbine interstage pressure too low
7	Main refrigerator compressor buffer tank pressure too high
8	The high current supply was on but has malfunctioned or gone off
9	The high voltage supply was on but has malfunctioned or gone off
10	The yellow alarm beacon is on
11	Operators have asked for site supervision to be transferred to the computer (an event, not an alarm)

dialing alarm system informs operators of a loss of electrical power. In addition, this system monitors a watchdog timer which must be continually reset by the computer. If it is not reset, the system notifies the operators of a computer malfunction when the timer times out.

These features can be easily replicated in a utility installation. Furthermore, fault-tolerant computing systems are already available for industrial automation and process monitoring and control³⁰. The capital cost of the computing equipment, transducers and storage peripherals is insignificant compared to the total cost of the installation, so duplication of those devices to increase reliability can be justified easily.

The hard-wired alarms function through the operation of conventional a.c. relay chains as in standard 'ladder diagram' alarm configurations. Experience indicates that the use of a.c. relays is not a wise choice where the control power to the site is susceptible to voltage sags. Power interruptions as short as one or two cycles can cause a relay to trip out and shut down the entire system, despite the fact that the interruption itself is of little consequence to the operation of the plant. The power transmission system has been designed, however, to be able to continue carrying its full power even after loss of all external refrigeration, as described in the section 'Abnormal and emergency conditions'.

Electrical excitation system

The 60 Hz electrical excitation system is designed to test the cables and terminations with simultaneous current and voltage up to and beyond the emergency rating. This is achieved by means of resonant circuits which require the expenditure of little power³¹. The simplified circuit used is shown in Figure 17. The current source on the upper left is simply a capacitor bank isolated from ground which tunes a loop formed of the two cable inner conductors into parallel resonance at 60 Hz. An equal and opposite current is induced in the loop formed by the outer conductors. Due to the leakage flux at the terminations the outer conductor current would normally be a little less than the inner conductor current. To adjust the balance between the currents in the cable conductors a small power supply is coupled to the outer conductor loop, this is shown on the right in Figure 17 (compensation supply). In power engineering terms this supply enables the zero sequence component of a three-phase system to be simulated. The compensation supply can be seen in Figure 2. The inner conductor voltage is derived by tuning the cable capacitance into series resonance by means of a variable inductor shown in the lower left portion of Figure 17. All the service requiring power at the inner conductor potential, such as instrumentation and glycol circulating pumps, are supplied with 115 V via a transformer with 100 kV primary to secondary insulation.

The performance of the 60 Hz excitation system is summarized in Table 6. Great care was taken in the design of the impulse test to avoid damage to refrigeration and control equipment in the event of a line-to-ground failure during the impulse. This problem is worse for superconducting cables because of the large stored energy needed to test a long cable. The Marx generator stores 150 kJ at 1 MV. The general arrangement of the test is shown in Figure 18. Deep wells were sunk at the west end to provide efficient grounds. Before the impulse test an additional well was placed at the refrigeration equipment building. By means of computer simulation the voltage transient was calculated at the equipment building assum-

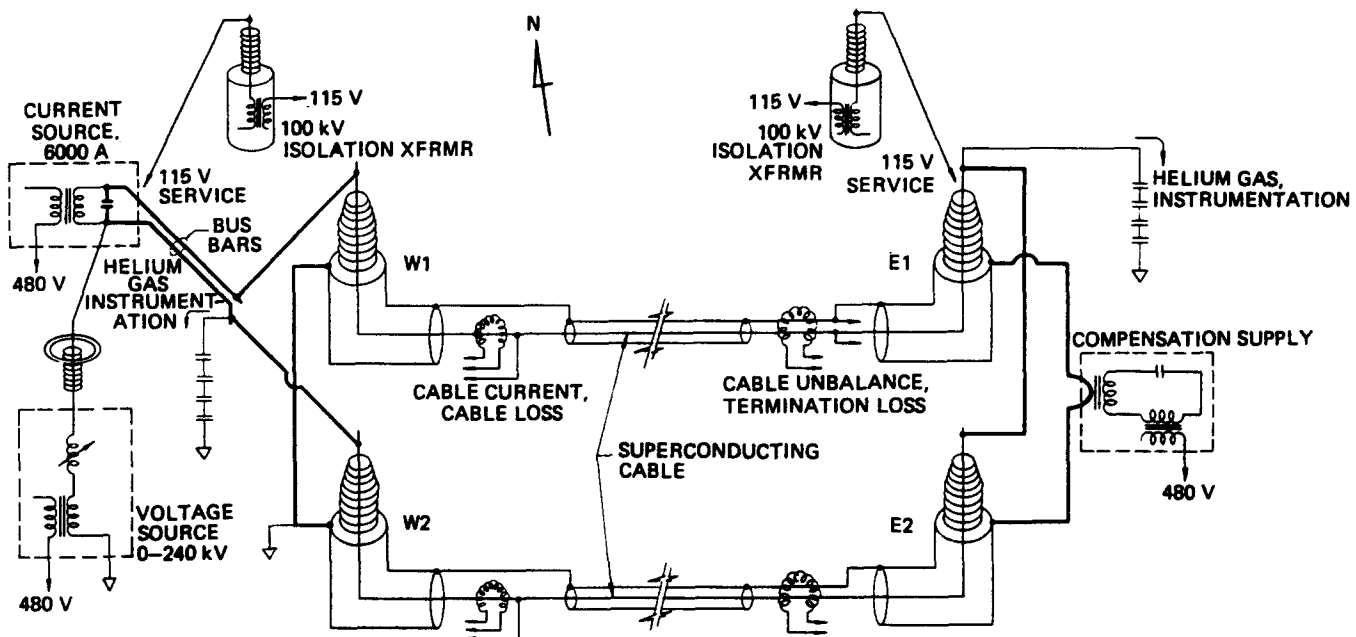


Figure 17 Simplified version of the high power test circuit. The inner conductors of the cables are short-circuited at the east end and a capacitor located at the west end tunes the loop to parallel resonance at 60 Hz. An equal and opposite current is induced in the loop formed by the outer conductors. Small adjustments of the outer conductor current are made by the compensation supply at the east end. The capacitance of the inner conductor loop is tuned into series resonance at 60 Hz by the voltage supply, thus permitting simultaneous voltage and current excitation of the cables with virtually no real power dissipation

ing failures at various places on the cable. The system shown is designed to keep the transient ground voltage at the equipment building to < 500 V for any worst case failure of the cables or terminations. Originally it had been intended to isolate all metal pipes and wires which connected the west pad to the equipment building. However, it was not feasible to design a ground break in the vacuum insulated helium piping. All other piping and electrical circuits were insulated at the ground break by the use of insulated flanges and optical links for the electrical circuits. A circuit analysis indicated that the transient ground voltages would last $< 1 \mu s$, so the time constant formed by the inductance of the helium pipe and the ground resistance at the equipment building was raised to $\approx 7 \mu s$ by means of metal toroidal cores clamped around the pipes. This problem was avoided in the eighth run which was performed after the cold-box was placed close to the west terminations, thus obviating the need for a cold transfer pipe to cross the ground-break.

The north cable was connected to the Marx generator at the west end and to a special terminating impedance at the east end. The impedance was tailored using a circuit simulation on the computer to achieve the best approximation of the desired impulse test waveform. The simulation also indicated that the worst case fault would be a flashover from the west termination to ground.

Table 6 Summary of 60 Hz excitation system (all values correspond to a cable current of 4100 A and simultaneous voltage of 80 kV to ground (330 MVA per cable))

Current source capacitance bank for resonance (F)	0.144
Current source voltage (V)	74
Compensation supply: unbalanced current range adjustment (A)	4 - 70
Voltage source current (A)	1.6
480 V feeder power to current source (kVA)	12
480 V feeder power to voltage source (kVA)	3.5

Under these conditions, at a peak waveform normalized to 1000 kV the fault current would be 60 kA. The voltage on the parasitic transmission line formed by the cable outer conductor to ground (which is terminated by 0.64Ω resistors at each end, see Figure 8) would be 22.5 kV or 40 MV m^{-1} on the insulation. With respect to a virtual ground the west end pad would rise to 37 kV (0.8 μs width to 50% points) and the equipment building ground would rise to 500 V.

Conclusions

The results presented in this Paper cover a four year operating period of the prototype superconducting power transmission system. The observed cryogenic and electrical performance data are the most comprehensive ever reported for such a system. These data are thus relevant to a determination of the desirability of further development of this technology.

The application of superconducting cables is in long distance, high power transmission circuits. They can be seen as an alternative for high voltage overhead lines in situations where aerial lines are prohibited for aesthetic reasons or for lack of right-of-way. The performance of the test system at Brookhaven has been compared to earlier systems studies¹³. The technical projections made earlier have been confirmed by the performance of the prototype system. The performance in many ways exceeded the designers' expectations: for example, it was not anticipated originally that life tests with unattended operation would prove feasible at this early stage of development.

Technical work still remains to be done before the technology is ready for actual electric utility company use. For example, the Brookhaven prototype does not include a joint. Three types of joints must be developed and tested: simple cable to cable splice, cooling loop to cooling loop transition and refrigeration connection point.

Much of the technology developed for the four

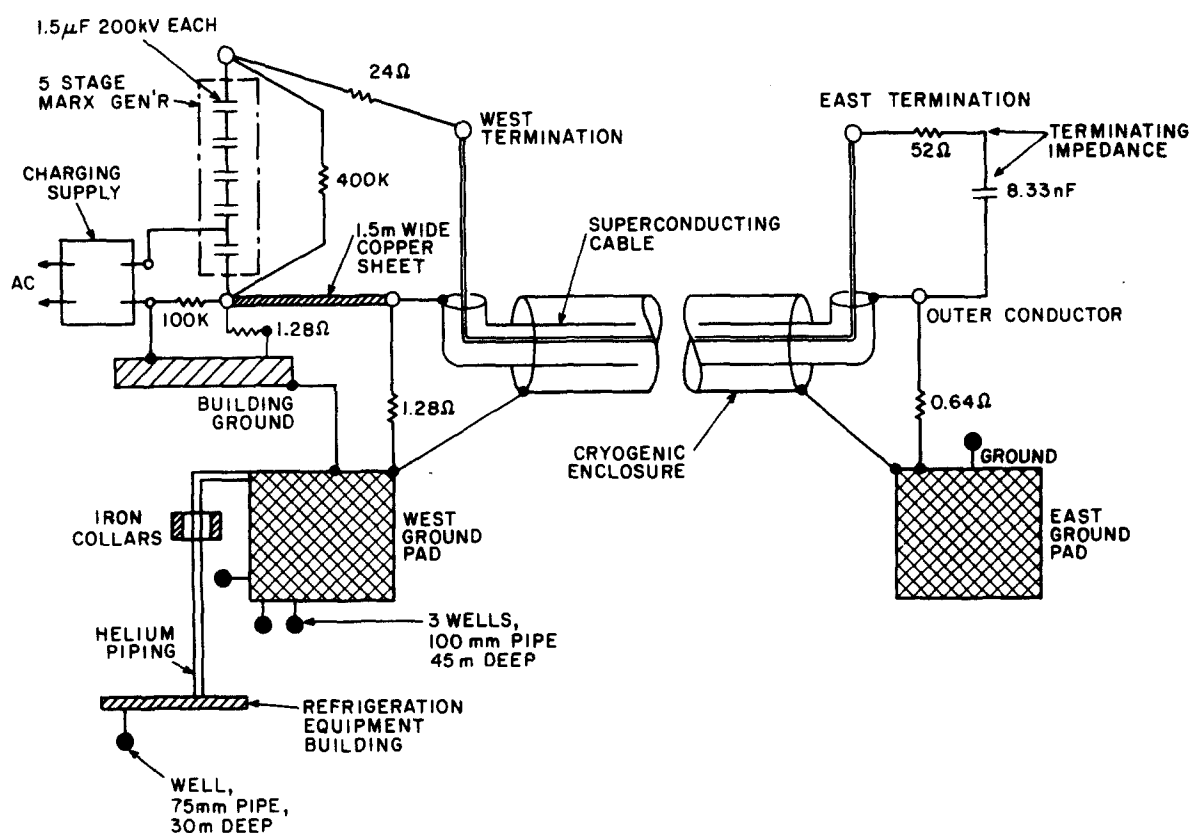


Figure 18 Simplified diagram of the test circuit for impulse testing

terminations of the Brookhaven prototype is applicable to these designs. In fact, a cable to cable joint has been designed in detail, but construction will depend on the future course of the project. Other technical problems of interest include methods of fast cool-down and warm-up and coolant storage during repairs to a cooling loop.

In addition to the technical development still required, the future commercialization of the technology will require the transfer of expertise to the commercial manufacturing sector. In particular, high voltage cable companies must acquire experience in making flexible superconducting cables, as in many ways the detailed construction departs significantly from conventional practice. There is no doubt that improvements can still be made in the conductor design for transmission applications. Very little work has gone into the methods of mass production of superconductors; a situation which is not likely to change until there is a rising demand.

Whether such a demand arises for a transmission cable superconductor clearly depends on the future course of development. The next period would cover the remaining technical problems discussed above as well as the technology transfer process. It is not the technical problems which will decide future progress but rather the complicated issue of how to proceed from the present prototype, which has demonstrated technical feasibility, to the commercial manufacture and use of the technology. Electric utility companies rightly require very detailed knowledge of the reliability, cost, operation and maintenance of any component installed in a utility system. To acquire such information a development programme would be needed which would probably be more expensive than the one that resulted in the present state-of-the-art. The funding of such a programme is complicated by the fact that the probable market for the technology is in routes 25 km in length. Obviously, a shorter length would be installed in any commercial demonstration project

meant to obtain the data needed to verify the proper system performance in a utility application, and thus it would not generate profit. Who pays for it in that case? Although a commitment by the government seems essential, it seems unlikely that it would totally underwrite the next phase without a consortium of potential builders and users sharing the cost.

Acknowledgements

The successful completion and testing of the prototype superconducting power transmission system is testimony to the skills of many craftsmen, technicians, engineers and scientists at Brookhaven and other cooperating institutions, both public and private. The financial support and encouragement of the Office of Electric Energy Systems of the US Department of Energy, and its predecessors, is gratefully acknowledged.

References

- 1 Forsyth, E.B. Underground power transmission by superconducting cable, *BNL 50325* (1972)
- 2 Forsyth, E.B. et al. Factors influencing the choice of superconductor in ac power transmission applications *Proc Applied Superconductivity Conf IEEE*, Pub no 72CH0682-5 TABSC (1972) 202
- 3 Forsyth, E.B. et al. Flexible superconducting power cables *IEEE Trans PAS* (1973) 92(2) 494
- 4 Forsyth, E.B. The developmental progress leading to the installation of a thousand feet of superconducting cable *Proc ICEC 9 Butterworths*, Guildford, UK (1982) 202
- 5 Forsyth, E.B. The 60 Hz performance of superconducting power transmission cables rated for 333 MVA per phase *IEEE Trans PAS*, (1984) 103(8) 2023
- 6 Muller, A.C. Properties of plastic tapes for cryogenic power cable insulation *Nonmetallic Materials and Composites at Low Temperatures* (Eds. A.F. Clark, R.P. Reed and G. Hartwig) Plenum Press, NY, USA (1979) 339
- 7 Gazzana-Priaroggia, P. et al. A brief review of the theory of

- paper lapping of a single-core high-voltage cable *Proc IEE* (1961) **108**(C) 25
- 8 **Morgan, G.H. and Muller, A.C.** Bending behaviour of lapped plastic EHV cable *IEEE International Symposium on Electrical Insulation* IEEE Pub 80 CH14969 (1980)
 - 9 **Morgan, G.H., Schauer, F. and Thomas, R.A.** An improved 60 Hz superconducting power transmission cable *IEEE Trans Magn* (1981) **MAG 17** 157
 - 10 **Garber, M.** A 10 m Nb₃Sn cable for 60 Hz power transmission *IEEE Trans Magn* (1979) **MAG 15** 155
 - 11 **Bussiere, J.F., Kovachev, V., Klamut, C. and Suenaga, M.** Nb₃Sn conductors for ac power transmission: electrical and mechanical characteristics *Proc 2nd ICMC, Adv Cryo Eng* Plenum Press, NY, USA (1978) **24** 449
 - 12 **Bussiere, J.F., Garber, M. and Shen, S.** The temperature dependence of ac losses and self-field critical currents in Nb₃Sn *App Phys Letters* (1974) **25** 756
 - 13 **Forsyth, E.B. and Thomas, R.A.** Operational test results of a prototype superconducting power transmission systems and their extrapolation to the performance of a large system *IEEE Trans Pow Del* (1986) **PWRD-1** (1) 10
 - 14 **Ward, D.A., Maddock, B.J. and Kyte, W.S.** Electromagnetic field and AC power loss enhancement at edges of adjacent strips in a superconducting cable *Cryogenics* (1979) **19** 339
 - 15 **Meats, R.J.** Pressurized-helium breakdown at very low temperatures *Proc IEE* (1972) **119** 760
 - 16 **Horii, K., Kosaki, M., Pearmain, A.J. and McNerney, A.J.** Correlation of electrical breakdown of supercritical helium in short gaps with partial discharge in cable samples *Cryogenics* (1983) **23** 102
 - 17 **Morgan, G.H., Jensen, J.E., McNerney, A.J., Minati, K.F. and Schmidt, R.D.** A horizontal cryogenic bushing for the termination of an ac superconducting power transmission line *Adv Cryo Eng* Plenum Press, NY, USA (1982) **27** 185
 - 18 **Schauer, F.** A capacitance-graded cryogenic high voltage bushing for vertical or horizontal mounting *Cryogenics* (1984) **24** 90
 - 19 **Forsyth, E.B., Mulligan, G.A., Beck, J.W. and Williams, J.A.** The technical and economic feasibility of superconducting power transmission: a case study *IEEE Trans PAS* (1975) **PAS-94** 161
 - 20 **Forsyth, E.B.** Cryogenic engineering for the Brookhaven power transmission project *Cryogenics* (1977) **17** 3
 - 21 **Morgan, G.H. and Jensen, J.E.** Counterflow cooling of a transmission line by supercritical helium *Cryogenics* (1977) **17** 257
 - 22 Philadelphia Electric Company (for the U.S. Department of Energy) Evaluation of the economical and technological viability of various underground transmission systems for long feeds to urban load areas, Report HCP/T)2055/1 (1977)
 - 23 **Jensen, J.E. and Minati, K.F.** The evolution of a cryogenic enclosure for a superconducting power transmission cable. Paper 77-HT-75 presented at ASME 17th National Heat Transfer Conference, Salt Lake City, Utah, USA (1977)
 - 24 **Forsyth, E.B. and Gibbs, R.J.** The Brookhaven superconducting cable test facility *IEEE Trans Mag* (1977) **MAG-13** 172
 - 25 **Gibbs, R.J.** Supercritical helium refrigerator to cool flexible superconducting power transmission cables *Adv Refrig Low Temp Commission A1*, 11R (1978)
 - 26 **Harison, W.E., Jr, Mille, A.C. Jr. and Shofner, F.M.** Principles and performance of a new aerosol detector in cryogenic systems *Cryogenics* (1978) **18** 363
 - 27 **Gusewell, D. and Haebel, E.U.** Current leads for refrigerator-cooled large superconducting magnets *Proc ICEC 3 IPC Science & Technology Press*, Guildford, UK (1970) 187
 - 28 **Eber, N., Quack, H. and Schmid, C.** Gas bearing turbines with dynamic gas bearings and their application in helium refrigerators *Cryogenics* (1978) **18** 585
 - 29 **Thomas, R.** Automated data acquisition for large cryogenic systems *Adv Cryo Eng* Plenum Press, NY, USA (1984) **29** 911
 - 30 **Serlin, O.** Fault-tolerant systems in commercial applications *Computer* (1984) **17**(8) 19
 - 31 **Forsyth, E.B., McNerney, A.J. and Meth, M.** Load excitation at the superconducting cable test facility *Proc 7th Symposium of the US/USSR Technical Exchange Committee on Superconducting Power Transmission* Moscow, USSR (1979) BNL Pub 26641